Hindawi
Advances in High Energy Physics
Volume 2019, Article ID 5393491, 12 pages
https://doi.org/10.1155/2019/5393491

Research Article

Parameterizing Dark Energy Models and Study of Finite Time Future Singularities

Tanwi Bandyopadhyay [1] **and Ujjal Debnath** [2]

[1] *Department of Mathematics, Adani Institute of Infrastructure Engineering, Ahmedabad-382421, Gujarat, India*
[2] *Department of Mathematics, Indian Institute of Engineering Science and Technology, Shibpur, Howrah-711103, India*

Correspondence should be addressed to Tanwi Bandyopadhyay; tanwib@gmail.com

Received 1 November 2018; Revised 1 March 2019; Accepted 21 March 2019; Published 9 April 2019

Academic Editor: Antonio J. Accioly

A review on spatially flat D-dimensional Friedmann-Robertson-Walker (FRW) model of the universe has been performed. Some standard parameterizations of the equation of state parameter of the dark energy models are proposed and the possibilities of finite time future singularities are investigated. It is found that certain types of these singularities may appear by tuning some parameters appropriately. Moreover, for a scalar field theoretic description of the model, it was found that the model undergoes bouncing solutions in some favorable cases.

1. Introduction

In order to avoid the initial singularity problem [1], a competitive alternative structure is proposed to the standard inflationary description. This is called the big bounce scenario ([2–10]). In this framework, the universe initially contracts continuously up to an initial narrow state with a nonzero minimal radius and then transforms to an expanding phase [11]. This means that the initial singularity is replaced by a bounce and consequently the cosmic equation of state (EoS) parameter crosses the phantom divide line (from $\omega < -1$ to $\omega > -1$).

On the other hand, various cosmological observations indicate the current cosmic acceleration ([12–21]). To explain this phenomenon in the homogeneous and isotropic universe, it is necessary to assume a component of matter with large negative pressure, called dark energy. Since the inception of this concept, a wide variety of phenomenological models have been proposed as the most suitable candidate of dark energy. Among them, the cosmological constant provides plausible answers but suffers from the fine-tuning problem. This issue has forced researchers to probe models having time-dependent equation of state parameter for the dark energy component. A simple classification of these models could be as follows:

(1) Cosmological constant ($\omega \equiv p/\rho = -1$)

(2) Dark energy with ω = constant $\neq -1$ [cosmic strings ($\omega = -1/3$), domain walls ($\omega = -2/3$)].

(3) Dynamical dark energy ($\omega = \omega(z) \neq$ constant) (i.e., quintessence, Chaplygin gas, k-essence, braneworld) ([22–30])

(4) Dark energy with $\omega(z) < -1$ [scalar-tensor theory, phantom models] ([31, 32])

The reconstruction problem for dark energy is reviewed in [33] in much detail (see also the references therein). Recently, in the literature [34], the possibilities of future singularities have been studied in the framework of Modified Chaplygin Gas filled universe and conditions of bounce were investigated. In this work, we provide more general results in terms of the possibilities of finite time future singularities in the context of a D-dimensional Friedmann-Robertson-Walker universe by imposing five standard parameterizations of the dark energy equation of state parameter. Different aspects of dark energy models have been studied so far to reconcile standard cosmological scenario with observations but no work has been done to the parameterization of these models in view of investigating the finite time future singularities.

The paper is organized as follows. In Section 2, we state the governing equations of the metric in the D-dimensional universe. In Section 3, the descriptions for the major physical

quantities are provided in the backdrop of five different parameterization models both analytically and graphically. In Section 4, the possibilities of future singularities are examined for these five models and the possible restrictions for certain type of singularity are shown in tabular form. In Section 5, the bouncing universe is described in the five parameterization models and, finally, we end with a short discussion in Section 6.

2. D-Dimensional Friedmann-Robertson-Walker Universe

We consider the D-dimensional spatially flat Friedmann-Robertson-Walker universe, given by [34]

$$ds^2 = -dt^2 + a^2(t)\, d\Omega^2 \tag{1}$$

where $a(t)$ is the scale factor and $d\Omega^2$ is the metric for the $(D-1)$-dimensional space. The field equations together with the energy conservation equation can be obtained as (assuming $8\pi G = c = 1$)

$$H^2 = \frac{2\rho}{(D-1)(D-2)} \tag{2}$$

$$\dot{H} + H^2 = -\frac{(D-1)\, p + (D-3)\, \rho}{(D-1)(D-2)} \tag{3}$$

and

$$\dot{\rho} + (D-1)\, H(\rho + p) = 0 \tag{4}$$

Here $H = \dot{a}/a$ denotes the Hubble parameter. In the following section and subsequent subsections, we will examine different parameterizations of dark energy models and attain analytical as well as graphical expressions of some physical entities involved in the process.

3. Dark Energy as Scalar Field for Various Parameterization Models

By considering scalar field ϕ with the potential $U(\phi)$, the effective Lagrangian [34] is given by

$$L_\phi = \frac{\dot{\phi}^2}{2} - U \tag{5}$$

So the energy density and pressure take the form

$$\rho = \frac{\dot{\phi}^2}{2} + U \tag{6}$$

$$p = \frac{\dot{\phi}^2}{2} - U \tag{7}$$

The kinetic energy for the field is given by

$$\dot{\phi}^2 = (1+\omega)\, \rho \tag{8}$$

where $\omega = p/\rho$. One can always write $\dot{\phi} = \phi' \dot{z}$, where the prime denotes differentiation with respect to redshift $z = 1/(1+a)$. With the help of (2), we have

$$\phi' = \sqrt{\frac{(D-1)(D-2)(1+\omega)}{2}}\, \frac{1}{1+z} \tag{9}$$

The scalar potential associated with the field is given by

$$U = \frac{1}{2}(1-\omega)\, \rho \tag{10}$$

In the next subsections, we will investigate the scalar field and its potential in different well-known parameterization models. A detailed review of different dark energy models can be found in [35].

3.1. Model I: Linear Parameterization. Here we assume the linear equation of state [36] $\omega = \omega(z) = \omega_0 + \omega_1 z$. Here ω_0 and ω_1 are constants. Using (4), the energy density of the model then gives rise to

$$\rho = \rho_0\, (1+z)^{(D-1)(1+\omega_0-\omega_1)}\, e^{(D-1)\omega_1 z} \tag{11}$$

Here ρ_0 is the present value of the energy density. The pressure of the fluid then becomes

$$p = (\omega_0 + \omega_1 z)\, \rho_0\, (1+z)^{(D-1)(1+\omega_0-\omega_1)}\, e^{(D-1)\omega_1 z} \tag{12}$$

Then (9) reduces to

$$\phi' = \sqrt{\frac{(D-1)(D-2)}{2}}\, \frac{\sqrt{1+\omega_0+\omega_1 z}}{1+z} \tag{13}$$

which on further integration gives rise to the scalar field as

$$\phi = \phi_0 + \sqrt{2(D-1)(D-2)} \left[\sqrt{1+\omega_0+\omega_1 z} - M \tan^{-1}\left(\frac{\sqrt{1+\omega_0+\omega_1 z}}{M} \right) \right] \tag{14}$$

where $M = \sqrt{\omega_1 - \omega_0 - 1}$. Also (10) changes to

$$U = \frac{1}{2}(1-\omega_0-\omega_1 z)\, \rho_0\, (1+z)^{(D-1)(1+\omega_0-\omega_1)}\, e^{(D-1)\omega_1 z} \tag{15}$$

We draw the variations of energy density ρ, pressure p, EoS parameter $\omega(z)$, Hubble parameter H, potential $U(\phi)$, and the scalar field ϕ with the variation in z in Figures 1(a)–1(f), respectively. Figure 1(g) shows the variation of $U(\phi)$ with ϕ. We observe that ρ, H, and ϕ decrease as z decreases. p and ω decrease from positive level to negative level as z decreases. $U(\phi)$ first increases up to certain value of z and then decreases as z decreases. Also $U(\phi)$ decreases as ϕ increases.

3.2. Model II: Chevallier-Polarski-Linder (CPL) Parameterization. In the Chevallier-Polarski-Linder (CPL) parameterization model, the equation of state is given by [37, 38] $\omega = \omega(z) = \omega_0 + \omega_1 (z/(1+z))$. Here again ω_0 and ω_1 are constants.

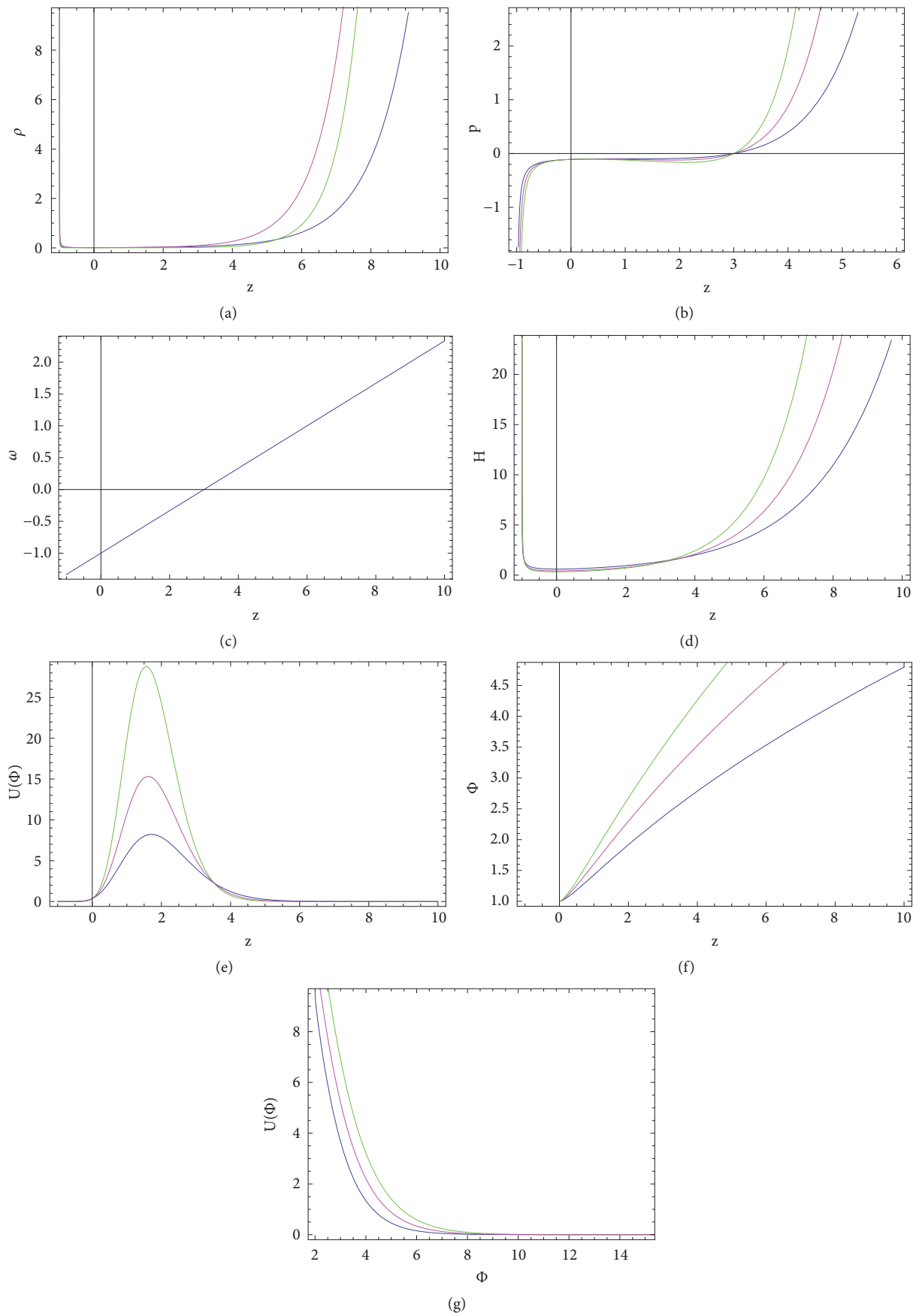

FIGURE 1: (a), (b), (c), (d), (e), and (f) show the variation of energy density ρ, pressure p, EoS parameter $\omega(z)$, Hubble parameter H, potential $U(\phi)$, and the scalar field ϕ with the variation in z for the *Linear* parameterizations. (g) shows the variation of $U(\phi)$ with ϕ. Different colored paths are obtained for different values of D.

With these, the expressions of energy density, pressure, scalar field, and the potential become

$$\rho = \rho_0 (1+z)^{(D-1)(1+\omega_0+\omega_1)} e^{-(D-1)\omega_1 z/(1+z)} \tag{16}$$

$$p = \left(\omega_0 + \omega_1 \frac{z}{1+z}\right) \rho_0 (1+z)^{(D-1)(1+\omega_0+\omega_1)} \cdot e^{-(D-1)\omega_1 z/(1+z)} \tag{17}$$

$$\phi = \phi_0 + \sqrt{2(D-1)(D-2)} \left[\sqrt{1+\omega_0+\omega_1} \cdot \log\left\{ (1+\omega_0+\omega_1)\sqrt{1+z} + \sqrt{1+\omega_0+\omega_1}\sqrt{(1+\omega_0)(1+z)+\omega_1 z} \right\} - \sqrt{(1+\omega_0)+\frac{\omega_1 z}{1+z}} \right] \tag{18}$$

and

$$U = \frac{1}{2}\left(1-\omega_0-\omega_1\frac{z}{1+z}\right)\rho_0 (1+z)^{(D-1)(1+\omega_0+\omega_1)} \cdot e^{-(D-1)\omega_1 z/(1+z)} \tag{19}$$

We draw the variations of energy density ρ, pressure p, EoS parameter $\omega(z)$, Hubble parameter H, potential $U(\phi)$, and the scalar field ϕ with the variation in z in Figures 2(a)–2(f), respectively. Figure 2(g) shows the variation of $U(\phi)$ with ϕ. We observe that ρ, H, and $U(\phi)$ first decrease up to $z = 0$ as z decreases and then sharply increase as z decreases. But p first increases up to $z = 0$ as z decreases and then sharply decreases as z decreases but keeps the negative level. ω decreases as z decreases and always keeps negative sign. ϕ increases as z decreases. Also $U(\phi)$ decreases as ϕ increases.

3.3. Model III: Jassal-Bagla-Padmanabhan (JBP) Parameterization. For the Jassal-Bagla-Padmanabhan (JBP) parameterization model, the equation of state changes to [39] $\omega = \omega(z) = \omega_0 + \omega_1(z/(1+z)^2)$, where ω_0 and ω_1 are constants. The following expressions are subsequently obtained as

$$\rho = \rho_0 (1+z)^{(D-1)(1+\omega_0)} e^{(D-1)\omega_1 z^2/2(1+z)^2} \tag{20}$$

$$p = \left[\omega_0 + \omega_1 \frac{z}{(1+z)^2}\right] \rho_0 (1+z)^{(D-1)(1+\omega_0)} \cdot e^{(D-1)\omega_1 z^2/2(1+z)^2} \tag{21}$$

$$\phi = \phi_0 + \sqrt{\frac{(D-1)(D-2)}{2}} \left[-\sqrt{1+\omega_0+\frac{\omega_1 z}{(1+z)^2}} + \frac{\sqrt{\omega_1}}{2}\tan^{-1}\left\{ \frac{\sqrt{\omega_1}(z-1)}{\sqrt{\omega_1 z+(1+\omega_0)(1+z)^2}} \right\} + \sqrt{1+\omega_0}\log\left\{ \omega_1 + 2(1+\omega_0)(1+z) + 2\sqrt{1+\omega_0}\sqrt{\omega_1 z+(1+\omega_0)(1+z)^2} \right\} \right] \tag{22}$$

$$U = \frac{1}{2}\left[1-\omega_0-\omega_1\frac{z}{(1+z)^2}\right]\rho_0 (1+z)^{(D-1)(1+\omega_0)} \cdot e^{(D-1)\omega_1 z^2/2(1+z)^2} \tag{23}$$

We draw the variations of energy density ρ, pressure p, EoS parameter $\omega(z)$, Hubble parameter H, potential $U(\phi)$, and the scalar field ϕ with the variation in z in Figures 3(a)–3(f), respectively. Figure 3(g) shows the variation of $U(\phi)$ with ϕ. We observe that ρ, H, and $U(\phi)$ first decrease up to $z = 0$ as z decreases and then sharply increase as z decreases. But p first increases up to $z = 0$ as z decreases and then sharply decreases as z decreases but keeps the negative level. ω first increases up to certain value of z and then sharply decreases but keeps negative sign. ϕ decreases as z decreases. Also $U(\phi)$ increases as ϕ increases.

3.4. Model IV: Alam-Sahni-Saini-Starobinsky (ASSS) Parameterization. In the Alam-Sahni-Saini-Starobinsky (ASSS) parameterization model, the equation of state parameter has the expression [40, 41]

$$\omega = \omega(z) = -1 + \frac{A_1(1+z)+2A_2(1+z)^2}{3\left[A_0+A_1(1+z)+A_2(1+z)^2\right]} \tag{24}$$

where, A_0, A_1, and A_2 are constants. In this case, the physical parameters ρ, p, ϕ, and U become

$$\rho = \rho_0 \left[\frac{A_0+A_1(1+z)+A_2(1+z)^2}{A_0+A_1+A_2}\right]^{(D-1)/3} \tag{25}$$

$$p = \left[-1+\frac{A_1(1+z)+2A_2(1+z)^2}{3\left\{A_0+A_1(1+z)+2A_2(1+z)^2\right\}}\right] \cdot \rho_0 \left[\frac{A_0+A_1(1+z)+A_2(1+z)^2}{A_0+A_1+A_2}\right]^{(D-1)/3} \tag{26}$$

$$\phi = \phi_0 + \sqrt{\frac{(D-1)(D-2)}{6}} \int \sqrt{\frac{2A_2+A_1/(1+z)}{A_0+A_1(1+z)+A_2(1+z)^2}}\, dz \tag{27}$$

$$U = \left[1-\frac{A_1(1+z)+2A_2(1+z)^2}{6\left\{A_0+A_1(1+z)+A_2(1+z)^2\right\}}\right] \cdot \rho_0 \left[\frac{A_0+A_1(1+z)+A_2(1+z)^2}{A_0+A_1+A_2}\right]^{(D-1)/3} \tag{28}$$

We draw the variations of energy density ρ, pressure p, EoS parameter $\omega(z)$, Hubble parameter H, potential $U(\phi)$, and the scalar field ϕ with the variation in z in Figures 4(a)–4(f), respectively. Figure 4(g) shows the variation of $U(\phi)$ with ϕ. We observe that ρ, H, ϕ, and $U(\phi)$ decrease as z decreases. p increases as z decreases but keeps negative sign. ω first decreases up to certain value of z and then increases as z decreases. Also $U(\phi)$ increases as ϕ increases.

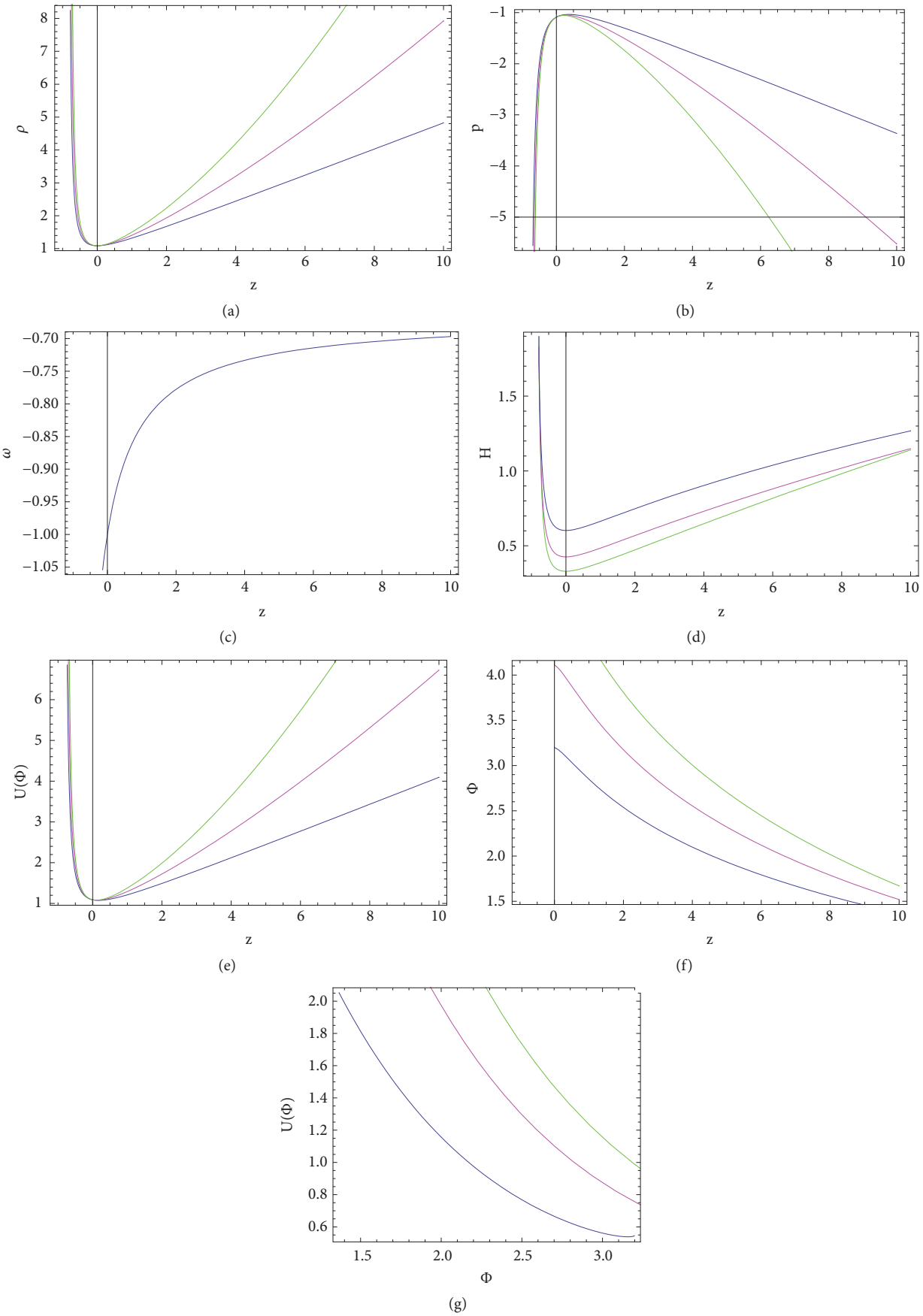

FIGURE 2: (a), (b), (c), (d), (e), and (f) show the variation of energy density ρ, pressure p, EoS parameter $\omega(z)$, Hubble parameter H, potential $U(\phi)$, and the scalar field ϕ with the variation in z for the *CPL* parameterizations. (g) shows the variation of $U(\phi)$ with ϕ. Different colored paths are obtained for different values of D.

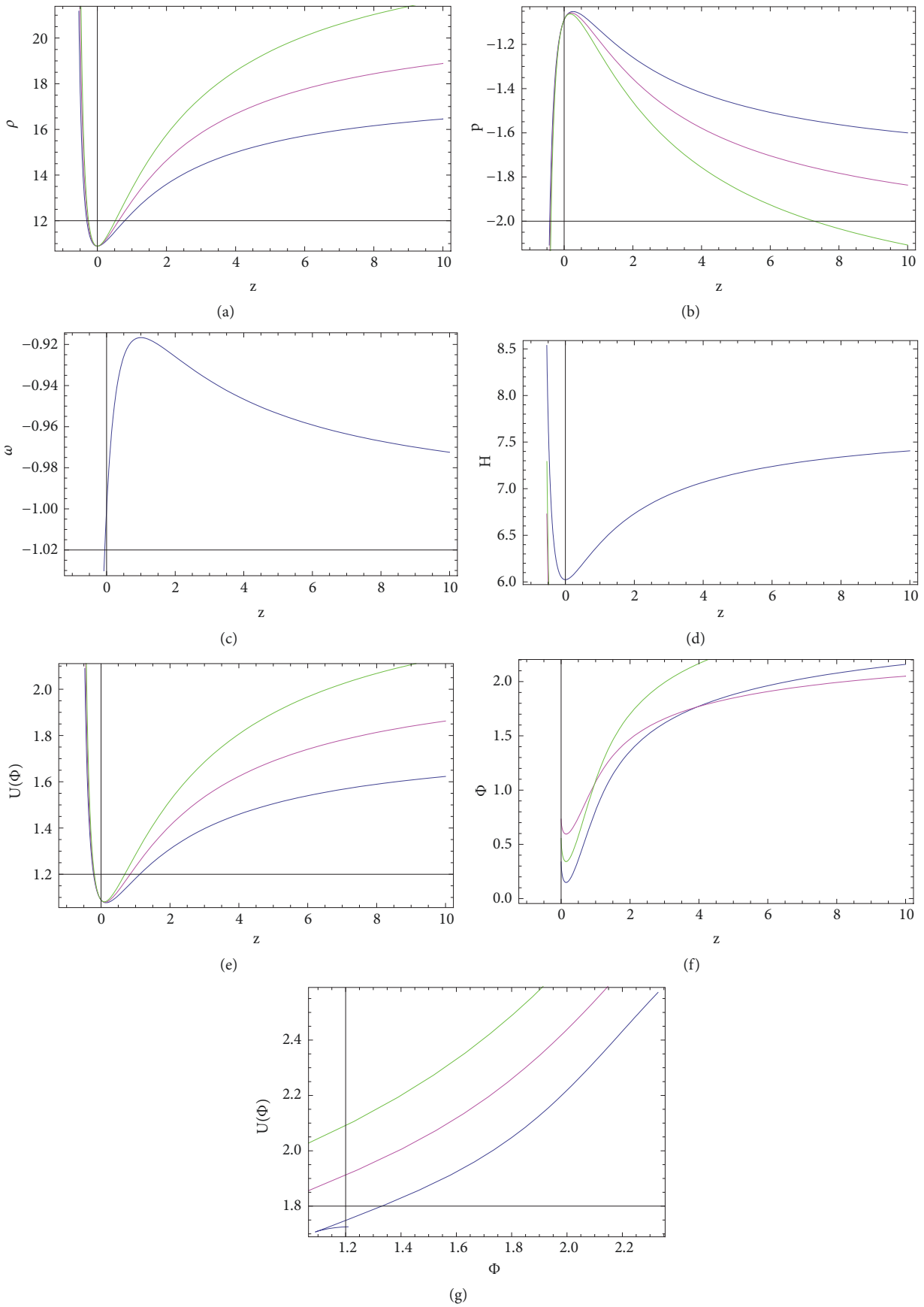

FIGURE 3: (a), (b), (c), (d), (e), and (f) show the variation of energy density ρ, pressure p, EoS parameter $\omega(z)$, Hubble parameter H, potential $U(\phi)$, and the scalar field ϕ with the variation in z for the *JBP* parameterizations. (g) shows the variation of $U(\phi)$ with ϕ. Different colored paths are obtained for different values of D.

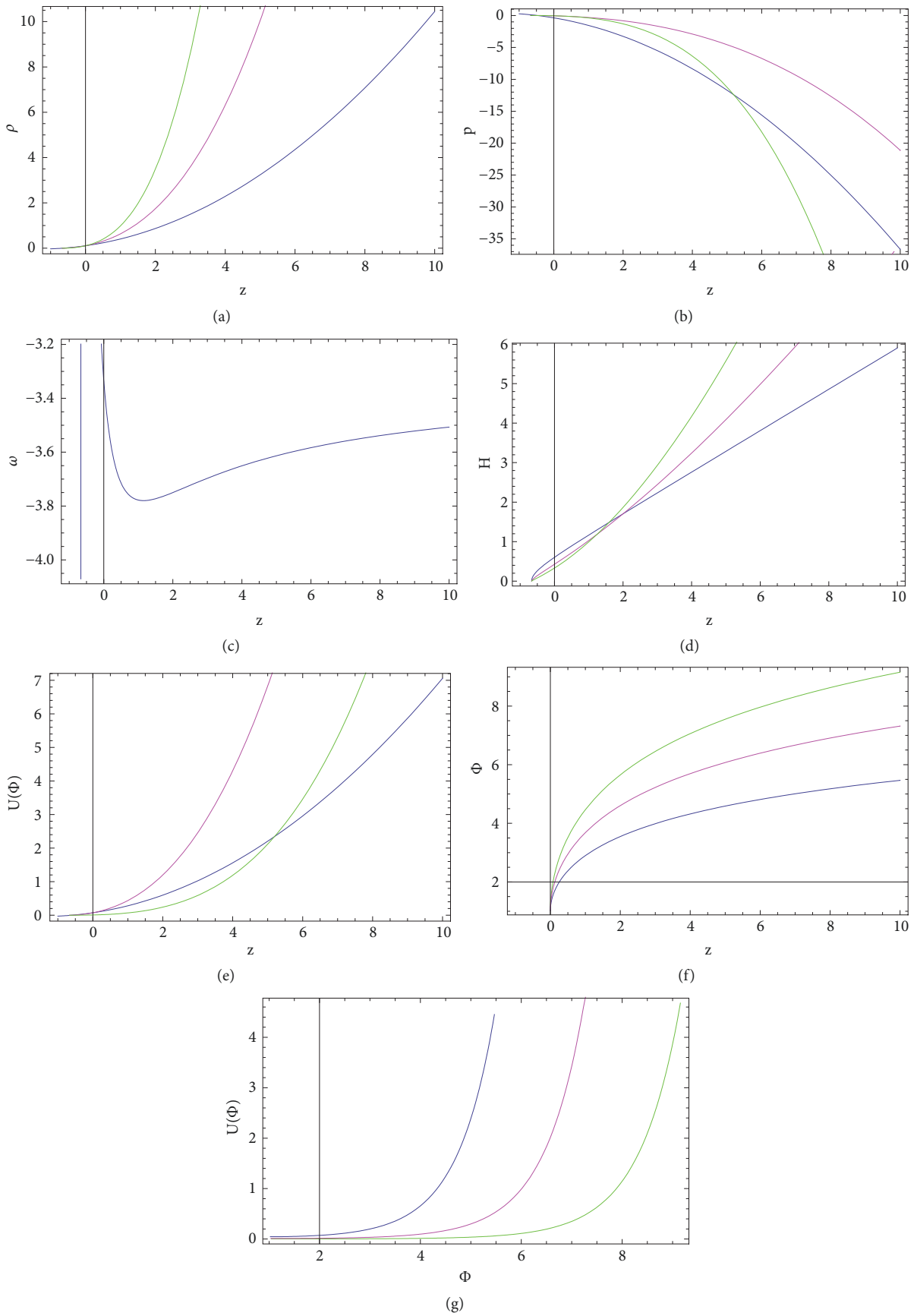

FIGURE 4: (a), (b), (c), (d), (e), and (f) show the variation of energy density ρ, pressure p, EoS parameter $\omega(z)$, Hubble parameter H, potential $U(\phi)$, and the scalar field ϕ with the variation in z for the *ASSS* parameterizations. (g) shows the variation of $U(\phi)$ with ϕ. Different colored paths are obtained for different values of D.

Table 1

Singularity/Model	Linear	CPL	JBP	ASSS	Efstathiou
Type I (Big Rip)	$1+\omega_0-\omega_1<0$	$\omega_1>0$	$\omega_1>0$	No	$\omega_1>0$
Type II (Sudden)	No	No	No	No	No
Type III	No	No	No	No	No
Type IV	No	No	No	${A_1}^2 \geq 4A_0A_2$	No

3.5. Model V: Efstathiou Parametrization. Here, in Efstathiou parametrization model, the equation of state takes the form [42, 43] $\omega = \omega(z) = \omega_0 + \omega_1 \log(1+z)$, where again ω_0 and ω_1 are constants. This gives rise to the following terms:

$$\rho = \rho_0 (1+z)^{(D-1)(1+\omega_0)} e^{((D-1)\omega_1/2)[\log(1+z)]^2} \tag{29}$$

$$p = \left[\omega_0 + \omega_1 \log(1+z)\right] \rho_0 (1+z)^{(D-1)(1+\omega_0)} \cdot e^{((D-1)\omega_1/2)[\log(1+z)]^2} \tag{30}$$

$$\phi = \phi_0 + \frac{\sqrt{2(D-1)(D-2)}}{3\omega_1} \left[1+\omega_0+\omega_1\log(1+z)\right]^{3/2} \tag{31}$$

$$U = \frac{1}{2}\left[1-\omega_0-\omega_1\log(1+z)\right] \rho_0 (1+z)^{(D-1)(1+\omega_0)} \cdot e^{((D-1)\omega_1/2)[\log(1+z)]^2} \tag{32}$$

We draw the variations of energy density ρ, pressure p, EoS parameter $\omega(z)$, Hubble parameter H, potential $U(\phi)$, and the scalar field ϕ with the variation in z in Figures 5(a)–5(f), respectively. Figure 5(g) shows the variation of $U(\phi)$ with ϕ. We observe that ρ, H, and $U(\phi)$ first decrease up to certain value of z as z decreases and then sharply increase as z decreases. But p first decreases from positive level to negative level and then slightly increases and then sharply decreases as z decreases but keeps the negative sign. ω decreases from positive level to negative level as z decreases. ϕ decreases as z decreases. Also $U(\phi)$ increases as ϕ increases.

4. Analysis of Future Singularities

The future singularities can be classified in the following ways [44, 45]:

(i) Type I (big rip): for $t \longrightarrow t_s$, $a \longrightarrow \infty$, $\rho \longrightarrow \infty$, and $|p| \longrightarrow \infty$

(ii) Type II (sudden): for $t \longrightarrow t_s$, $a \longrightarrow a_s$, $\rho \longrightarrow \rho_s$, and $|p| \longrightarrow \infty$

(iii) Type III: $t \longrightarrow t_s$, $a \longrightarrow a_s$, $\rho \longrightarrow \infty$, and $|p| \longrightarrow \infty$

(iv) Type IV: for $t \longrightarrow t_s$, $a \longrightarrow a_s$, $\rho \longrightarrow 0$, and $|p| \longrightarrow 0$

where t_s, a_s, and ρ_s are constants with $a_s \neq 0$.

Table 1 shows the restrictions on the parameters involved in the five parameterization models for the occurrence of the future singularities.

5. Bouncing Universe

The initial singularity in the cosmological models can be avoided by introducing the nonsingular bouncing models. In these models, a universe undergoing a "bounce" stage attains a minimum after a collapsing phase and then subsequently expands. During the collapse, the scale factor $a(t)$ decreases $[\dot{a}(t) < 0]$ and, during the expanding phase, it increases $[\dot{a}(t) > 0]$. At the bounce point, $t = t_b$, the minimal necessary condition (may not be sufficient) is $\dot{a}(t) = 0$ and $\ddot{a}(t) > 0$ for $t \in (t_b - c, t_b) \cup (t_b, t_b + c)$ for small $c > 0$. For a nonsingular bounce $a(t_b) \neq 0$.

In the current study, the bouncing universe can be viewed in different parameterizing models from Figures 6(a)–6(j), where the evolution of the scale factor $a(t)$ and the EoS parameter ω are shown with respect to time t for each model. For the bouncing phase, the scale factor first decreases and then increases in order that the universe enters into the hot Big Bang era immediately after the bounce. The nature of the equation of state parameters has been presented in the figures. The figures clearly show bouncing solutions for linear, CPL, JBP, ASSS, and Efstathiou models with a minimal nonzero scale factor $a(t)$.

6. Discussion

In this work, we have considered the D-dimensional flat FRW model of the universe in the background of some well-known parametrization of dark energy models like linear, CPL, JBP, ASSS, and Efstathiou. By considering the scalar field model as these parametrizations of dark energy, we found the energy density, pressure, scalar field, and corresponding potential in terms of the redshift z. In model I (linear), we have drawn the variations of energy density ρ, pressure p, EoS parameter $\omega(z)$, Hubble parameter H, potential $U(\phi)$, and the scalar field ϕ with the variation in z in Figures 1(a)–1(f), respectively. Figure 1(g) shows the variation of $U(\phi)$ with ϕ. We have seen that ρ, H, and ϕ decrease as z decreases. p and ω decrease from positive level to negative level as z decreases. $U(\phi)$ first increases up to certain value of z and then decreases as z decreases. Also $U(\phi)$ decreases as ϕ increases.

In model II (CPL), we have drawn the variations of energy density ρ, pressure p, EoS parameter $\omega(z)$, Hubble parameter H, potential $U(\phi)$, and the scalar field ϕ with the variation in z in Figures 2(a)–2(f), respectively. Figure 2(g) shows the variation of $U(\phi)$ with ϕ. We have seen that ρ, H, and $U(\phi)$ first decrease up to $z = 0$ as z decreases and then sharply increase as z decreases. But p first increases up to $z = 0$ as z decreases and then sharply decreases as z decreases but keeps the negative level. ω decreases as z decreases and always keeps

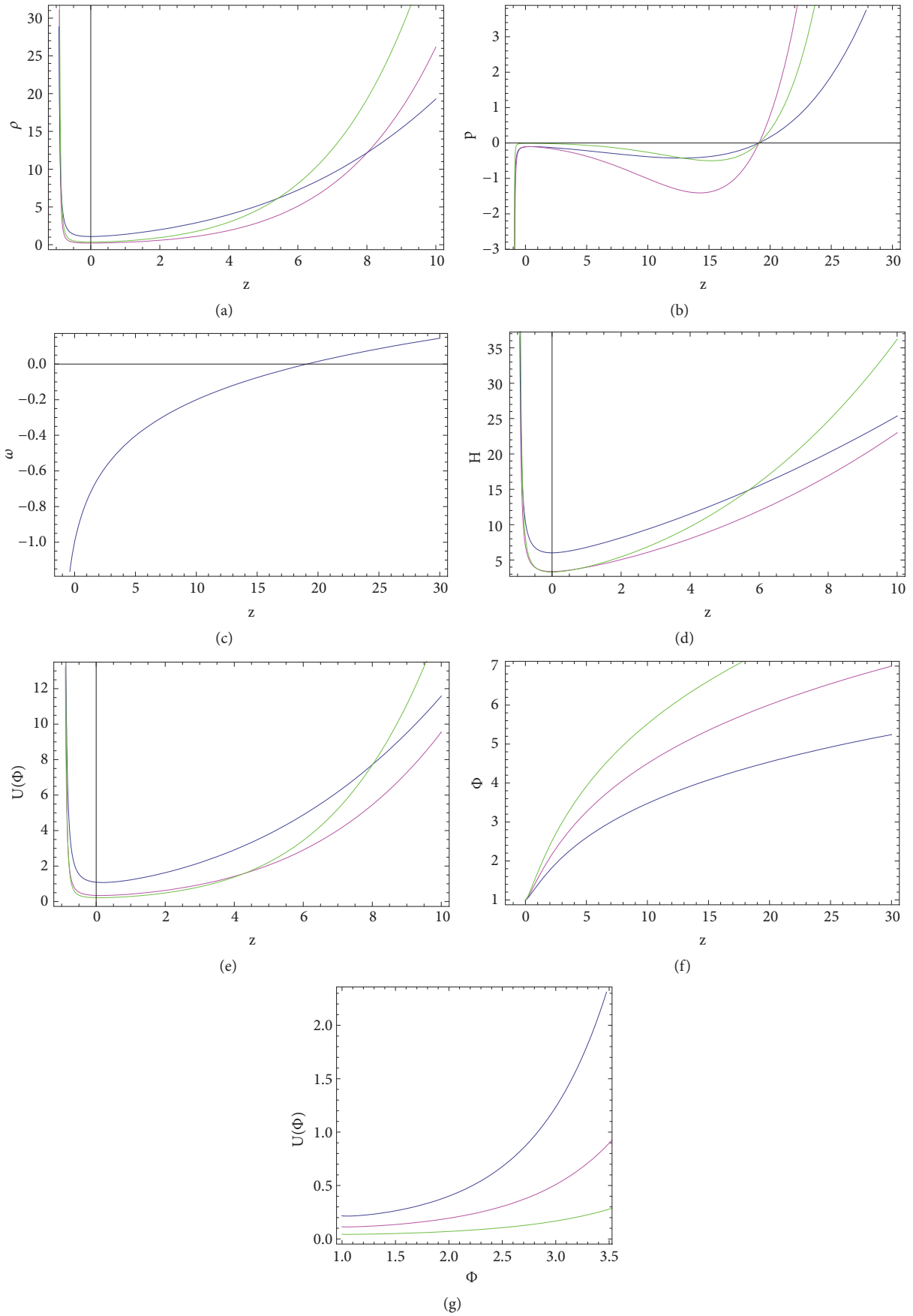

FIGURE 5: (a), (b), (c), (d), (e), and (f) show the variation of energy density ρ, pressure p, EoS parameter $\omega(z)$, Hubble parameter H, potential $U(\phi)$, and the scalar field ϕ with the variation in z for the *Efstathiou* parameterizations. (g) shows the variation of $U(\phi)$ with ϕ. Different colored paths are obtained for different values of D.

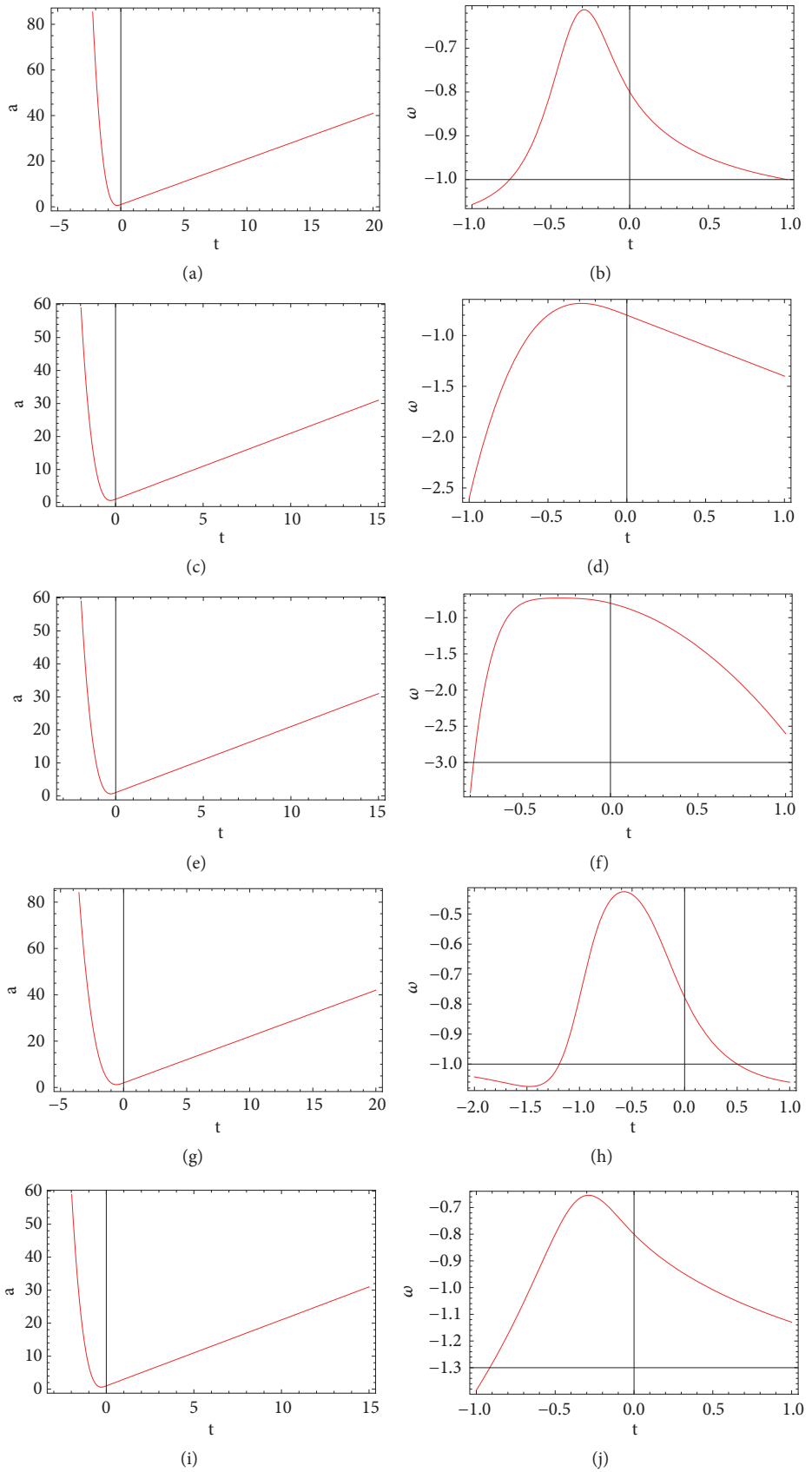

FIGURE 6: (a) and (b) (linear), (c) and (d) (CPL), (e) and (f) (JBP), (g) and (h) (ASSS), and (i) and (j) (Efstathiou) show the variation of scale factor $a(t)$ ((a), (c), (e), (g), and (i)) and EoS parameter ω ((b), (d), (f), (h), and (j)) with the variation in cosmic time t for the different parameterization models.

negative sign. ϕ increases as z decreases. Also $U(\phi)$ decreases as ϕ increases.

In model III (JBP), we have drawn the variations of energy density ρ, pressure p, EoS parameter $\omega(z)$, Hubble parameter H, potential $U(\phi)$, and the scalar field ϕ with the variation in z in Figures 3(a)–3(f), respectively. Figure 3(g) shows the variation of $U(\phi)$ with ϕ. We have seen that ρ, H, and $U(\phi)$ first decrease up to $z = 0$ as z decreases and then sharply increase as z decreases. But p first increases up to $z = 0$ as z decreases and then sharply decreases as z decreases but keeps the negative level. ω first increases up to certain value of z and then sharply decreases but keeps negative sign. ϕ decreases as z decreases. Also $U(\phi)$ increases as ϕ increases.

In model IV (ASSS), we have drawn the variations of energy density ρ, pressure p, EoS parameter $\omega(z)$, Hubble parameter H, potential $U(\phi)$, and the scalar field ϕ with the variation in z in Figures 4(a)–4(f), respectively. Figure 4(g) shows the variation of $U(\phi)$ with ϕ. We have seen that ρ, H, ϕ, and $U(\phi)$ decrease as z decreases. p increases as z decreases but keeps negative sign. ω first decreases up to certain value of z and then increases as z decreases. Also $U(\phi)$ increases as ϕ increases.

In model V (Efstathiou), we have drawn the variations of energy density ρ, pressure p, EoS parameter $\omega(z)$, Hubble parameter H, potential $U(\phi)$, and the scalar field ϕ with the variation in z in Figures 5(a)–5(f), respectively. Figure 5(g) shows the variation of $U(\phi)$ with ϕ. We have seen that ρ, H, and $U(\phi)$ first decrease up to certain value of z as z decreases and then sharply increase as z decreases. But p first decreases from positive level to negative level and then slightly increases and then sharply decreases as z decreases but keeps the negative sign. ω decreases from positive level to negative level as z decreases. ϕ decreases as z decreases. Also $U(\phi)$ increases as ϕ increases.

Also the present work is designed to investigate the possibilities of finite time future singularities, that is, types I (big rip), II (sudden), III, and IV singularities. From Table 1, we observe that, for linear parametrization model, the type I (big rip) singularity occurs provided $1+\omega_0-\omega_1 < 0$, but types II-IV singularities cannot occur. For CPL parametrization model, the type I (big rip) singularity occurs provided $\omega_1 > 0$, but types II-IV singularities cannot occur. For JBP parametrization model, the type I (big rip) singularity occurs provided $\omega_1 > 0$, but types II-IV singularities cannot occur. For ASSS parametrization model, the types I-III singularities cannot occur; only type IV singularity occurs provided ${A_1}^2 \geq 4A_0A_2$. For Efstathiou parametrization model, the type I (big rip) singularity occurs provided $\omega_1 > 0$, but types II-IV singularities cannot occur.

Data Availability

The data used to support the findings of this study are included within the article in the references and therein.

Conflicts of Interest

The authors declare that there are no conflicts of interest regarding the publication of this paper.

Acknowledgments

The authors are thankful to IUCAA, Pune, for their warm hospitality where most of the work has been done during a visit under the Associateship Programme.

References

[1] A. Borde and A. Vilenkin, "Eternal inflation and the initial singularity," *Physical Review Letters*, vol. 72, no. 21, pp. 3305–3308, 1994.

[2] M. Novello and S. E. P. Bergliaffa, "Bouncing cosmologies," *Physics Reports*, vol. 463, no. 4, pp. 127–213, 2008.

[3] J.-L. Lehners, "Cosmic bounces and cyclic universes," *Classical and Quantum Gravity*, vol. 28, no. 20, Article ID 204004, 21 pages, 2011.

[4] Y. F. Cai and E. N. Saridakis, "Non-singular cyclic cosmology without phantom menace," *Journal of Cosmology*, vol. 17, pp. 7238–7254, 2011.

[5] J. Khoury, B. A. Ovrut, and J. Stokes, "The worldvolume action of kink solitons in AdS spacetime," *Journal of High Energy Physics*, vol. 8, p. 15, 2012.

[6] Y. Cai, D. A. Easson, and R. Brandenberger, "Towards a nonsingular bouncing cosmology," *Journal of Cosmology and Astroparticle Physics*, vol. 2012, no. 8, p. 20, 2012.

[7] M. Koehn, J. Lehners, and B. A. Ovrut, "Cosmological superbounce," *Physical Review D: Particles, Fields, Gravitation and Cosmology*, vol. 90, no. 2, Article ID 025005, 2014.

[8] Y. F. Cai and E. Wilson-Ewing, "Non-singular bounce scenarios in loop quantum cosmology and the effective field description," *Journal of Cosmology and Astroparticle Physics*, vol. 2014, article no. 1403, p. 8, 2014.

[9] S. D. Odintsov and V. K. Oikonomou, "ΛCDM Bounce Cosmology without ΛCDM: the case of modified gravity," *Physical Review D*, vol. 91, no. 6, Article ID 064036, 2015.

[10] S. D. Odintsov and V. K. Oikonomou, "Deformed matter bounce with dark energy epoch," *Physical Review D*, vol. 94, no. 6, Article ID 064022, 19 pages, 2016.

[11] Y. F. Cai, "Bouncing universe with quintom matter," *Journal of High Energy Physics*, vol. 2007, no. 10, article 071, 2007.

[12] A. G. Riess, A. V. Filippenko, and P. Challis, "Observational evidence from supernovae for an accelerating universe and a cosmological constant," *The Astronomical Journal*, vol. 116, p. 1009, 1998.

[13] A. G. Riess, L.-G. Strolger, J. Tonry et al., "Type la supernova discoveries at z>1 from the *Hubble Space Telescope*: evidence for past deceleration and constraints on dark energy evolution," *The Astrophysical Journal*, vol. 607, no. 2, p. 665, 2004.

[14] S. Perlmutter, G. Aldering, M. Della Valle et al., "Discovery of a supernova explosion at half the age of the Universe," *Nature*, vol. 391, no. 6662, pp. 51–54, 1998.

[15] S. Perlmutter, G. Aldering, and G. Goldhaber, "Measurements of Ω and Λ from 42 high-redshift supernovae," *The Astrophysical Journal*, vol. 517, p. 565, 1999.

[16] P. M. Garnavich, R. P. Kirshner, and P. Challis, "Constraints on cosmological models from Hubble space telescope observations of high-z supernovae," *The Astrophysical Journal*, vol. 493, no. 2, pp. L53–L57, 1998.

[17] C. L. Bennett, M. Halpern, and G. Hinshaw, "First-year *wilkinson microwave anisotropy probe (WMAP)** observations:

preliminary maps and basic results," *The Astrophysical Journal Supplement Series*, vol. 148, pp. 1–27, 2003.

[18] D. N. Spergel, L. Verde, and H. V. Peiris, "First year *Wilkinson Microwave Anisotropy Probe (WMAP)* observations: determination of cosmological parameters," *The Astrophysical Journal Supplement Series*, vol. 148, no. 1, pp. 175–194, 2003.

[19] L. Verde, F. Alan, H. Will et al., "The 2dF galaxy redshift survey: the bias of galaxies and the density of the universe," *Monthly Notices of the Royal Astronomical Society*, vol. 335, pp. 432–440, 2002.

[20] E. Hawkins, S. Maddox, S. Cole et al., "The 2dF galaxy redshift survey: correlation functions, peculiar velocities and the matter density of the Universe," *Monthly Notices of the Royal Astronomical Society*, vol. 346, no. 1, pp. 78–96, 2003.

[21] M. Tegmark, M. A. Strauss, M. R. Blanton et al., "Cosmological parameters from SDSS and WMAP," *Physical Review D*, vol. 69, no. 10, Article ID 103501, 26 pages, 2004.

[22] B. Ratra and P. J. E. Peebles, "Cosmological consequences of a rolling homogeneous scalar field," *Physical Review D: Particles, Fields, Gravitation and Cosmology*, vol. 37, no. 12, pp. 3406–3427, 1988.

[23] I. Zlatev, L. Wang, and P. J. Steinhardt, "Quintessence, cosmic coincidence, and the cosmological constant," *Physical Review Letters*, vol. 82, no. 5, pp. 896–899, 1999.

[24] A. Kamenshchik, U. Moschella, and V. Pasquier, "An alternative to quintessence," *Physics Letters B*, vol. 511, no. 2-4, pp. 265–268, 2001.

[25] F. C. Santos, M. L. Bedran, and V. Soares, "On the thermodynamic stability of the modified Chaplygin gas," *Physics Letters. B. Particle Physics, Nuclear Physics and Cosmology*, vol. 646, no. 5-6, pp. 215–221, 2007.

[26] C. Armendariz-Picon, V. Mukhanov, and P. J. Steinhardt, "Dynamical solution to the problem of a small cosmological constant and late-time cosmic acceleration," *Physical Review Letters*, vol. 85, no. 21, pp. 4438–4441, 2000.

[27] L. Randall and R. Sundrum, "Large mass hierarchy from a small extra dimension," *Physical Review Letters*, vol. 83, no. 17, pp. 3370–3373, 1999.

[28] L. Randall and R. Sundrum, "An alternative to compactification," *Physical Review Letters*, vol. 83, no. 23, pp. 4690–4693, 1999.

[29] C. Deffayet, G. Dvali, and G. Gabadadze, "Accelerated universe from gravity leaking to extra dimensions," *Physical Review D: Particles, Fields, Gravitation and Cosmology*, vol. 65, no. 4, Article ID 044023, 2002.

[30] V. Sahni and Y. Shtanov, "Braneworld models of dark energy," *Journal of Cosmology and Astroparticle Physics*, vol. 2003, no. 11, article 014, 2003.

[31] B. Boisseau, G. Esposito-Farèse, D. Polarski, and A. Starobinsky, "Reconstruction of a scalar-tensor theory of gravity in an accelerating universe," *Physical Review Letters*, vol. 85, no. 11, pp. 2236–2239, 2000.

[32] J. M. Cline, S. Jeon, and G. D. Moore, "The phantom menaced: constraints on low-energy effective ghosts," *Physical Review D: Particles, Fields, Gravitation and Cosmology*, vol. 70, Article ID 043543, 2004.

[33] V. Sahni and A. A. Starobinsky, "Reconstructing dark energy," *International Journal of Modern Physics D*, vol. 15, no. 12, pp. 2105–2132, 2006.

[34] S. D. Sadatian, "Rip singularity scenario and bouncing universe in a chaplygin gas dark energy model," *International Journal of Theoretical Physics*, vol. 53, pp. 675–684, 2014.

[35] K. Bamba, S. Capozziello, S. Nojiri, S. D. Odintsov, and K. Bamba, "Dark energy cosmology: the equivalent description via different theoretical models and cosmography tests," *Astrophysics and Space Science*, vol. 342, no. 1, pp. 155–228, 2012.

[36] A. R. Cooray and D. Huterer, "Gravitational lensing as a probe of quintessence," *The Astrophysical Journal*, vol. 513, no. 2, pp. L95–L98, 1999.

[37] M. Chevallier and D. Polarski, "Accelerating universes with scaling dark matter," *International Journal of Modern Physics D*, vol. 10, pp. 213–224, 2001.

[38] E. V. Linder, "Exploring the expansion history of the universe," *Physical Review Letters*, vol. 90, no. 9, Article ID 091301, p. 4, 2003.

[39] H. K. Jassal, J. S. Bagla, and T. Padmanabhan, "WMAP constraints on low redshift evolution of dark energy," *Monthly Notices of the Royal Astronomical Society*, vol. 356, p. L11, 2005.

[40] U. Alam, V. Sahni, T. D. Saini, and A. A. Starobinsky, "Is there supernova evidence for dark energy metamorphosis?" *Monthly Notices of the Royal Astronomical Society*, vol. 354, no. 1, pp. 275–291, 2004.

[41] U. Alam, V. Sahni, and A. A. Starobinsky, "The case for dynamical dark energy revisited," *Journal of Cosmology and Astroparticle Physics*, vol. 2004, no. 6, p. 8, 2004.

[42] G. Efstathiou, "Constraining the equation of state of the universe from distant Type Ia supernovae and cosmic microwave background anisotropies," *Monthly Notices of the Royal Astronomical Society*, vol. 310, no. 3, pp. 842–850, 1999.

[43] R. Silva, J. S. Alcaniz, and J. A. S. Lima, "On the thermodynamics of dark energy," *International Journal of Modern Physics D*, vol. 16, pp. 469–473, 2007.

[44] B. McInnes, "The dS/CFT correspondence and the big smash," *Journal of High Energy Physics*, vol. 2002, no. 8, article 029, 2002.

[45] S. Nojiri, S. D. Odintsov, and S. Tsujikawa, "Properties of singularities in the (phantom) dark energy universe," *Physical Review D: Particles, Fields, Gravitation and Cosmology*, vol. 71, Article ID 063004, 2005.